DOI: 10.1002/chem.200500078

Intramolecular Hydrogen-Bond-Assisted Planarization of Asymmetrically Functionalized Alternating Phenylene–Pyridinylene Copolymers

Muthalagu Vetrichelvan[a] and Suresh Valiyaveettil*[a, b]

Abstract: We report on the synthesis and characterization of a series of asymmetrically functionalized amphiphilic polymers with alternating π-donor units (e.g., substituted benzene) and π-acceptor units (e.g., pyridine) along the polymer backbone. The purpose of our present work involves incorporation of functional groups along the main chain to form intrachain hydrogen bonds, which promote planarization of the polymer backbone, and to fine-tune the optical properties. The structure–property relationship of polymers **P1**–**P6** was investigated by means of analytical methods, such as FTIR spectroscopy, ^{1}H and ^{13}C NMR spectroscopy, UV/Vis spectroscopy, fluorescence spectroscopy, gel permeation chromatography, thermogravimetric analysis, cyclic voltammetry, and X-ray powder diffraction. All polymers were soluble in common organic solvents, and the optical and fluorescence spectra of the polymers showed significant changes according to the formation (**P4**, **P5**) or absence (**P6**) of intramolecular hydrogen bonding along the polymer backbone. Moreover, the 2,6- or 3,5-linkage of the pyridine rings in **P5** and **P6**, respectively, reduced the conjugation along the polymer backbone and this is reflected in their optical properties. The optical properties of the polymers were influenced by the addition of acid (**P1**–**P6**), base (**P4**–**P6**), and metal ions (e.g., Cu^{2+}, Fe^{3+}, Ag^{+}, Ni^{2+}, Pd^{2+}, Mn^{2+}, Zn^{2+}, Mg^{2+}, and Pr^{3+}). Such polymers could be used in various applications, including sensors and stimuli-responsive displays.

Keywords: optical tuning · planarization · poly(paraphenylene) · pyridine · sensors · transition metals

Introduction

Conjugated polymers have received much attention in the past two decades owing to their potential applications in light-emitting diodes,[1–7] thin-film transistors,[1–2] chemical sensors,[8] as well as electronic and photonic devices.[9–11] The optoelectronic properties of conjugated polymers vary significantly depending on the degree of extended conjugation between the consecutive repeating units and the inherent electron densities on the polymer backbone.[12–14] Among them, conjugated pyridine-incorporated polymers have attracted much attention owing to the possibility of fine-tuning the optical properties by means of 1) the electron-accepting ability, 2) N-protonation, 3) N-oxidation, 4) N-alkylation, and 5) metal complexation.[15–29] π-Conjugated polymers that incorporate aryl heterocyclic units, such as pyridine, pyrrole, and thiophene rings, have been synthesized and employed in industrial applications.[30–34] The ladder-type polymers incorporated with pyrazines,[35] benzothiadazoles,[36]pyrroloimides,[37] pyridobisimidazoles,[38] and benzothiazole[39] that contain intramolecular hydrogen bonds along the polymer backbone are also known in the literature. One of the most important features of the pyridine-incorporated polymers is the high electron affinity of pyridine compared to phenylene-based polymers.[40] Furthermore, the use of a donor–acceptor system[41] and planarization of the polymer backbone by means of weak interactions (e.g., intrachain hydrogen bonds) allow us to fine-tune the optical and conducting properties of the polymers.[21–22]

Recently, a few reports have focused on the incorporation of pyridine into a conjugated polymer backbone.[27–29,42–46] Chemical sensors based on conjugated polymers are interesting owing to their high sensitivity.[8] The synthesis of conjugated polymers with bipyridine/phenanthroline moieties or crown ethers or a combination of both groups have already been reported in the literature.[8,15,46] Our research ef-

[a] Dr. M. Vetrichelvan, Prof. S. Valiyaveettil
Singapore-MIT Alliance, 4 Engineering Drive 3
National University of Singapore—117 576 (Singapore)
E-mail: chmsv@nus.edu.sg

[b] Prof. S. Valiyaveettil
Department of Chemistry, 3 Science Drive 3
National University of Singapore—117 543 (Singapore)
Fax: (+65) 6779-1691

Supporting information for this article is available on the WWW under http://www.chemeurj.org/ or from the author.

forts are focused on the synthesis and structure–property investigations of asymmetrically functionalized planar poly(paraphenylene)s (PPPs).[47–49] The target PPPs contain alternating functionalized phenylene rings and 2,5-, 2,6-, or 3,5-substituted pyridine rings on the polymer backbone.

Dodecyloxy groups are incorporated to increase the solubility and ordered packing through alkyl-chain crystallization. The intramolecular hydrogen bonds between the adjacent phenolic OH groups in **P4** and **P5** and the nitrogen atom of the pyridine ring help to planarize the polymer backbone. However, in polymer **P6**, no such intramolecular hydrogen bonds are expected. The optical properties of the polymer can be fine-tuned by protonation or alkylation of the nitrogen atom, deprotonation of the OH groups, and metal-ion complexation.

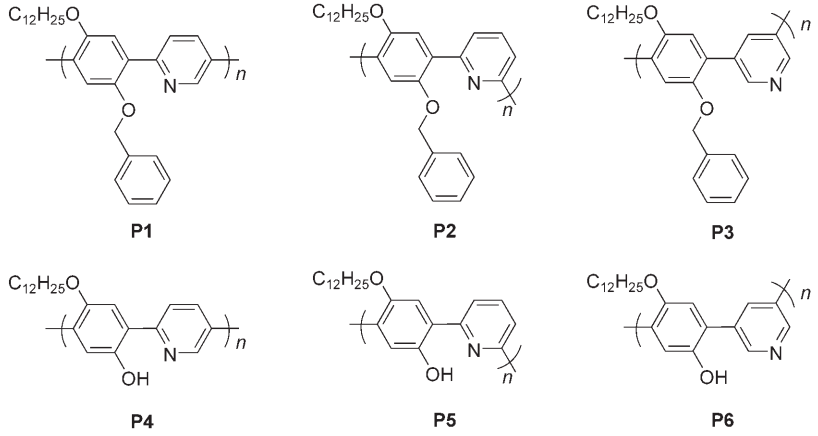

Results and Discussion

Synthesis and characterization: Recently, a simple oligomer of the target polymer was synthesized by our group. It demonstrated planarization of the rings owing to the formation of intramolecular hydrogen bonds.[50] The crystal structure of the oligomer (Figure 1) revealed the presence of hydrogen bonds between the hydroxyl groups and the pyridine nitrogen atoms. Interestingly, the torsion angle between the hydroquinol ring and the pyridine ring is reduced to 4.7°, which results in planarization of the molecule. Even though it is difficult to see a one-to-one structural correlation between oligomers and polymers, we incorporated such functional groups along the main chain of our target polymers to facilitate intramolecular hydrogen-bond-assisted planarization of the polymer backbone.

The general synthetic route to the target polymers (**P1** and **P4**) is outlined in Scheme 1. The monomer 1-benzyloxy-4-dodecyloxyphenyl-2,5-bis(boronic acid) (**5**) was synthesized from hydroquinone following a reported procedure.[42] 2,5-Dibromohydroquinone (**2**) was obtained by bromination of hydroquinone with bromine in acetic acid.[51] Monoalkylation of **2** with dodecyl bromide in the presence of NaOH/EtOH at 45–50 °C gave compound **3**, which was benzylated to afford **4**. Compound **4** was reacted with *n*-butyllithium followed by quenching with triisopropyl borate and hydrolysis with hydrochloric acid to afford bis(boronic acid) **5**. All polymerizations were carried out by means of Suzuki polycondensation reactions[42–43,46] in a mixture (3:2 v/v) of toluene and aqueous potassium carbonate solution (2 M) containing 3.0 mol % [$Pd(PPh_3)_4$] with vigorous stirring at 85–90 °C for 72 h under a nitrogen atmosphere. After completion of the reaction, the polymer was precipitated from methanol. The target polymers, **P4**–**P6**, were prepared by debenzylation of a solution of **P1**–**P3** in $CHCl_3$/THF/EtOH under a hydrogen atmosphere with 10 % Pd/C as the catalyst. The resulting solution was filtered (silica gel/celite), concentrated, and refiltered. The residue was washed with methanol and dried to yield polymers **P4** and **P5**. In the case of polymer **P6**, the filtrate was concentrated to afford a solid polymer.

The molecular weights of the polymers were measured by using gel permeation chromatography (GPC) with THF as the eluant and polystyrene as the standard (Table 1). The observed values are relatively low with a polydispersity index of 1.1–1.4. This may be attributable to the fractionation of soluble low-molecular-weight polymer in solution.

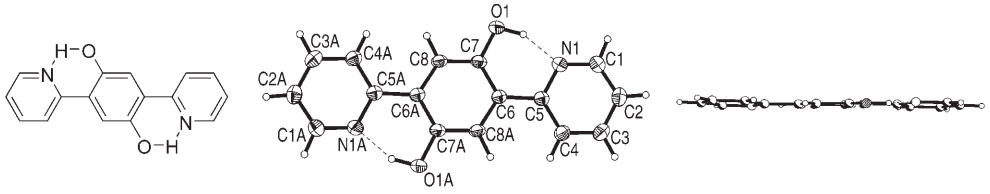

Figure 1. Molecular structure of the oligomer (left), and its crystal structure: top view (middle) and side view (right). Hydrogen bonds are marked as dotted lines.

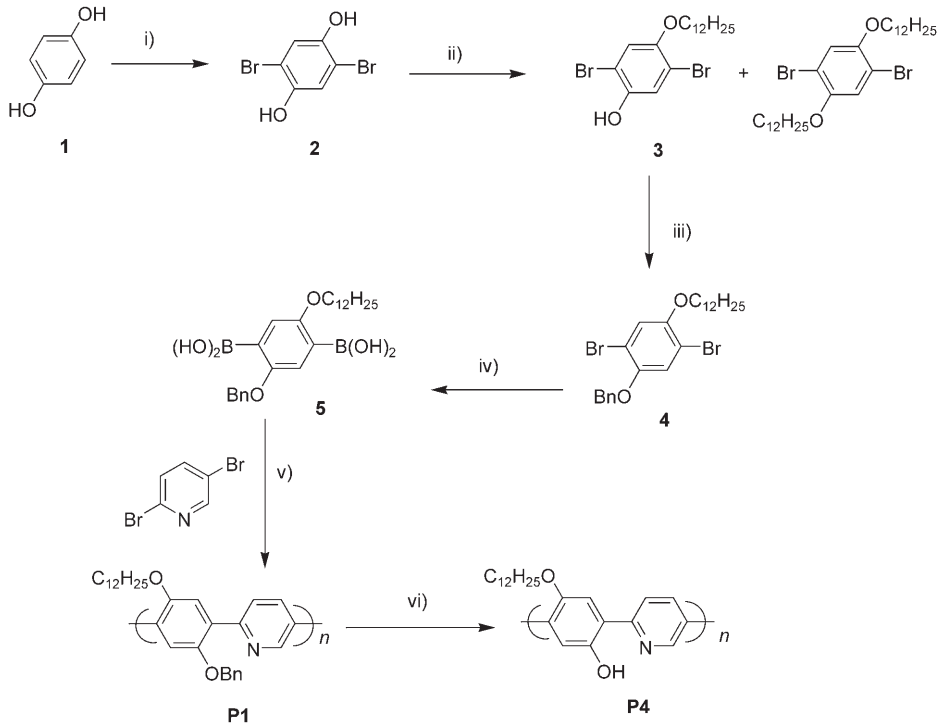

Scheme 1. Synthesis of polymers **P1** and **P4**: i) Br_2/AcOH, 80%; ii) NaOH/EtOH, $CH_3(CH_2)_{11}Br$, 45–50°C, 10 h, 65%; iii) K_2CO_3, $C_6H_5CH_2Br$, 50°C, 10 h, 90%; iv) *n*BuLi, THF, −78°C, triisopropyl borate, RT, 10 h, 70%; v) K_2CO_3 (2 M), toluene, $[Pd(PPh_3)_4]$ (3.0 mol%), reflux, 3 days; vi) H_2, 10% Pd/C, $CHCl_3$/EtOH/THF.

Table 1. Molecular weight and polydispersity index (PDI) of polymers **P1**–**P6** at room temperature.

Polymer	Color	M_n[a]	M_w[b]	PDI
P1	bright yellow	3265	3883	1.1
P2	yellow	4354	6421	1.4
P3	light brown	3659	5284	1.4
P4	dark brown	2234	2389	1.1
P5	dark brown	2642	3292	1.3
P6	dark brown	2357	2591	1.1

[a] Number-average molecular weight. [b] Weight-average molecular weight.

According to Müllen et al., the GPC results for rigid rod polymers, particularly polymers with polar groups, are not completely reliable with polystyrene standards, and the measured value is often lower than the actual molecular weight.[52] Moreover, the structure and properties of the low-molecular-weight PPPs may be similar to the oligomer discussed above rather than to the high-molecular-weight polymers. The obtained polymers **P1**–**P6** are soluble in common organic solvents, such as THF, chloroform, toluene, and trifluoroacetic acid.

All polymers (**P1**–**P6**) were characterized by means of FTIR, ^1H NMR, ^{13}C NMR, GPC, thermogravimetric analysis (TGA), and X-ray diffraction. The assignments of the ^1H and ^{13}C NMR peaks are given in the Experimental Section. For polymer **P1**, peaks assigned to protons on the pyridine rings were observed at $\delta \approx 9.0$, 8.2, and 8.1 ppm. Those of the phenylene ring protons appeared at $\delta = 7.9$ and 7.4 ppm. The -CH_2- signal of the benzyl group appeared at 5.2 ppm and -OCH_2- at 4.1 ppm. The remaining peaks at $\delta = 1.8$, 1.3, and 0.9 ppm were assigned to the hydrogen atoms on the aliphatic dodecyloxy groups. Data for polymers **P2**–**P3** were also in good agreement with the proposed structure. The NMR signals of the target polymers **P4**–**P6** appeared as broad signals, and it is expected that the polymer may contain head-to-head and head-to-tail units along the backbone.[42]

Thermal properties: The thermal stability of the polymers was evaluated by TGA with a heating rate of 10°C min^{-1} under a nitrogen atmosphere. Benzylated parent polymers **P1**–**P3** showed good thermal stability, and the onset degradation temperatures were in the range of 290–310°C (Figure 2). This decomposition corresponds to the degradation of the benzyl groups on the polymer backbone. The second onset temperature at 390–520°C corresponds to the decomposition of dodecyloxy groups and the polymer backbone. Thus, two-step degradations were observed for polymers **P1**–**P3**. For the target polymers **P4**–**P6**, decomposition temperatures were observed at 80 and 220°C; the first decomposition is attributed to evaporation

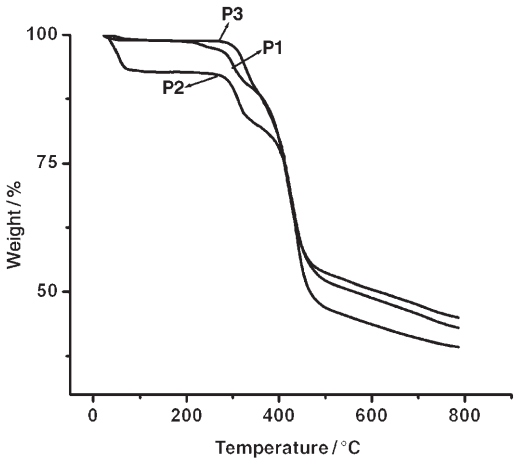

Figure 2. TGA traces of precursor polymers **P1**–**P3**. TGA data of **P4**–**P6** are given in the Supporting Information.

of the entrapped solvents from the polymer lattice. The second decomposition above 370 °C corresponds to the loss of dodecyloxy groups and the polymer backbone.

Electrochemical properties: The electrochemical behavior of polymers **P1**–**P6** was investigated by means of cyclic voltammetry (CV). The experiments were performed in a 0.1 M solution of Bu_4NClO_4 in acetonitrile, with a scan rate of 50 mV s^{-1} at room temperature under a nitrogen atmosphere. A glassy carbon electrode was coated with a thin polymer film and was used as the working electrode. Cyclic voltammograms of polymers **P1** and **P4** are shown in Figure 3, and the electrochemical data of the polymers **P1**–**P6** are summarized in Table 2.

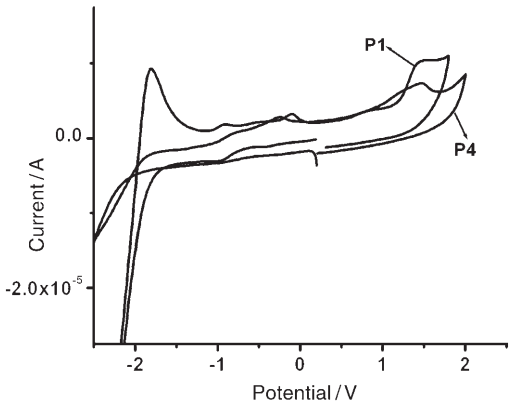

Figure 3. Cyclic voltammogram of a thin film of polymers **P1** and **P4** recorded with a glassy carbon electrode under a nitrogen atmosphere. CV traces of the other polymers are given in the Supporting Information.

Table 2. Electrochemical potentials and energy levels of polymers **P1**–**P6** at room temperature.[a]

Polymer	Band gap[b]	E_{ox} (onset) [V][c]	E_{red} (onset) [V][c]	HOMO [eV][d]	Calcd LUMO [eV][e]
P1	3.0	1.24	−1.85	5.68	−2.68
P2	3.1	0.96	–	5.40	−2.27
P3	3.3	–	–	–	–
P4	2.5	0.9	–	5.34	−2.84
P5	2.9	–	–	–	–
P6	3.2	1.00	–	5.44	−2.22

[a] Electrochemical data are not available for **P3** and **P5**. [b] Estimated from the onset wavelengths of the polymer in solution. [c] Estimated from cyclic voltammetry. [d] Calculated from the onset oxidation potential. [e] Because no reduction potentials were observed, they had to be derived from the band gap and the HOMO.

The appearance of multiple oxidation and reduction peaks is common to polymers containing electroactive groups such as pyridine rings. In the oxidation region, a peak was observed at ≈+1.3–1.5 V with reference to (Ag^+/Ag) and was assigned to the oxidation of the phenylene group (main polymer chain). Such oxidation potentials have been observed for other pyridine-containing copolymers,[16,42,46] and these values may be useful towards establishing the electron-transport properties. Additional oxidation peaks were observed at −0.1 and −0.4 V for **P1** and **P2**, respectively. The oxidation potential (E_{ox}) of **P1** is higher (1.52 V) than that of **P2** (1.32 V), which indicates that **P2** can be easily oxidized or *p* doped compared with **P1**. Consequently, HOMO and LUMO energy levels of **P2** were lower than those of **P1**.[53,54] For target polymers **P4** and **P6**, there was a slight difference in the oxidation potential compared with the precursor polymers **P1** and **P2**. Polymer **P4** exhibited an oxidation peak at +1.51 V and a small peak at −0.3 V. The strong interaction of the -$OC_{12}H_{25}$ groups with the counteranion of the supporting electrolyte (perchlorate) may be one of the reasons for the observed irreversibility.[46] Only **P1** showed a reduction peak at −2.1 V.

The observed band gaps for the phenylene–pyridinylene copolymers are generally 3.0–3.5 eV.[54] The calculated band gap for our polymers **P1**–**P6** are 3.0, 2.9, 3.3, 2.5, 2.9, and 3.2 eV, respectively.[55] The values of the band gap for the benzylated precursor polymers (**P1**–**P3**) are higher than those of the corresponding debenzylated target polymers (**P4**–**P6**), and the values for benzylated polymers, **P1**–**P3**, are comparable to the symmetrically functionalized PPP copolymers.[54] However, in the case of the debenzylated polymers (**P4**–**P6**), the band gaps are lower than 3.0 eV, except for **P6**, which contains *meta*-linked pyridine linkages on the polymer backbone. Thus, the functionalization and intramolecular hydrogen bonds facilitated a reduction in the size of the band gap to 2.5 and 2.8 eV for **P4** and **P5** polymers, respectively.

Optical properties

Absorption and emission spectroscopy: The absorption and emission properties of the polymers (**P1**–**P5** in chloroform and **P6** in methanol) are summarized in Table 3. The optical properties of the polymers in chloroform are dependent on the linkage (2,5-, 2,6-, or 3,5-) of the pyridyl rings and planarization of the polymer backbone that results from hydrogen bonding. From the structure of the oligomer (Figure 1), it is clear that intramolecular hydrogen bonding facilitates planarization of the molecule. The absorption spectra of the polymers showed two maxima located in the range λ_{max} = 270–300 nm and one above 300 nm. For polymers (**P1** and **P4**) with 2,5-substituted pyridine rings, the absorption maxima were observed at 384 and 425 nm, respectively, (Figure 4). For **P2** and **P5** with 2,6-substitution, the λ_{max} were blueshift-

Table 3. Absorption and emission wavelengths for the polymers **P1**–**P6** in chloroform.

	λ_{max} [nm]/E [eV]	ε_{max}	λ_{emiss} [nm]/E [eV]
P1	384/3.2	9.15×10^4	431/2.9
P2	359/3.5	13.04×10^4	402/3.1
P3	331/3.7	9.89×10^4	393/3.2
P4	425/2.9	4.83×10^4	503/2.5
P5	362/3.4	5.28×10^4	420/3.0
P6[a]	302/4.1	1.50×10^4	392/3.2

[a] Methanol or tetrahydrofuran.

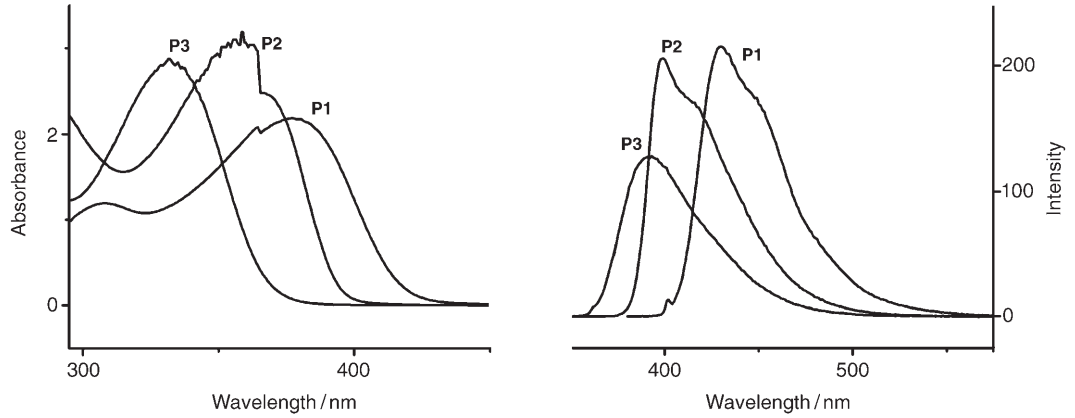

Figure 4. Absorption (left) and emission (right) spectra of polymers **P1**–**P3** in chloroform at room temperature. Absorbance and intensity have arbitrary units.

ed to 359 and 362 nm, respectively (Table 3). The latter is attributed to the low π-conjugation length on the polymer backbone because of the *meta*-linked pyridine rings.

The absorption maxima (λ_{max}) for polymers **P3** and **P6** with 3,5-substituted pyridine rings were blueshifted to 331 and 302 nm, respectively, implying a minimum π-conjugation length. It is also interesting to note that the λ_{max} for **P3** is higher than that for **P6**, which is presumably caused by intermolecular hydrogen-bond formation in the **P6** polymer lattice. This reduces the planarity and effective conjugation length along the polymer backbone in **P6**.

The target polymers (**P4**–**P6**) have higher λ_{max} values than the corresponding precursor polymers (**P1**–**P3**) with a $\Delta\lambda_{max}$ of 4–45 nm. The shift in the absorption maximum of precursor polymer **P1** to the target polymer **P4** was ≈41 nm. This large shift may be attributable to planarization of the polymer backbone, which is caused by the formation of intramolecular hydrogen bonds between the adjacent phenolic OH groups and the pyridine nitrogen atoms as seen in the crystal lattice of the oligomer (Figure 1). Moreover, the λ_{max} value of **P6** is significantly smaller than that observed for **P4**. This again confirms the role of intramolecular hydrogen bonding in the planarization of the polymer backbone. Also, the λ_{max} value of linear **P1** or **P4** is higher than that of the bent polymers **P2** and **P3** and the corresponding debenzylated polymers **P5** and **P6**. The FTIR spectra of the target polymers showed a sharp absorption in the region of 3437–3406 cm^{-1}, which indicates hydrogen-bond formation inside the polymer lattice. The value of λ_{max} for polymer **P4** in a polar solvent, such as tetrahydrofuran (THF, weak intramolecular hydrogen bond) is smaller (383 nm) than in the nonpolar solvent, chloroform (425 nm). This is only applicable for **P4**, and in all other cases there were no changes in the values of λ_{max} in different solvents. This may be attributable to the formation of strong intramolecular hydrogen bonds in nonpolar chloroform leading to high planarity and conjugation length.[37]

The emission spectra of the polymers (**P1**–**P6**) were recorded by exciting them at the maximum absorption wavelength observed from the corresponding UV-visible spectra of the polymers. All our polymers (**P1**–**P6**), except **P4**, emit in the blue region. However, polymer **P4** emits in the green region (Figure 5, Table 3). Absorption and emission spectra of **P1**–**P3** and **P4**–**P6** are given in Figures 4 and 5, respec-

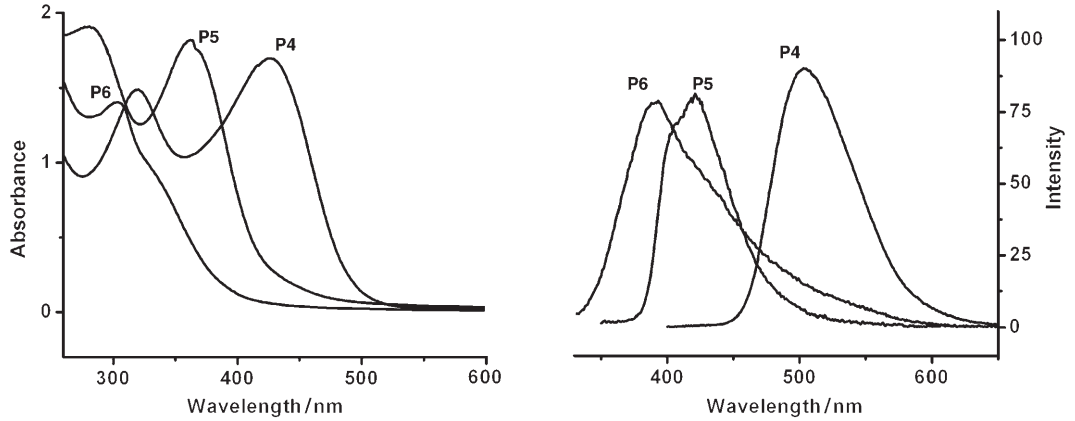

Figure 5. Absorption (left) and emission (right) spectra of polymers **P4**–**P6** in chloroform at room temperature. The observed blueshift in the maxima of **P6** and **P5** indicates less planarization for the polymer backbone. Absorbance and intensity have arbitrary units.

tively. Polymer **P4** emits in the green region ($\lambda_{max}=503$ nm) with a large Stokes shift of ≈ 72 nm. This may be attributable to the possibility of hydrogen-bond-assisted excited-state intramolecular proton transfer (ESIPT), as observed for other hydrogen-bonded oligomers and polymers.[57–61] Similar Stokes shifts were observed for **P5** and **P6** (Table 2). However, for the 2,6-substituted (**P2** and **P5**) and 3,5-substituted (**P3** and **P6**) polymers, the differences in λ_{emiss} are 18 and 1 nm, respectively. The difference in λ_{emiss} between **P2** and **P5** can also be explained by ESIPT, as described for 2,5-substituted polymers, (**P1** and **P4**) owing to the formation of hydrogen bonds between the phenolic OH group and the pyridine nitrogen atom. However, the reduction in the value may be caused by the *meta*-linked pyridine rings along the polymer chain. In the case of polymers **P3** and **P6**, intrachain hydrogen bonds cannot be formed owing to the 3,5-linkage of pyridine rings along the polymer chain and this may explain the insignificant difference in λ_{emiss} values. However, strong intermolecular hydrogen bonding is possible in the lattice of **P6**, which is insoluble in chloroform, but soluble in more polar solvents, such as methanol. The intermolecular hydrogen bonds also reduce the planarity of the polymer chain, as seen in the values of λ_{max} (Table 3). Polymer **P4** emits in the green region (503 nm) in chloroform and in the blue region (432 nm) in THF at the excitation wavelength of 365 nm. The other polymers did not show such solvatochromism. This again indicates the formation of strong intramolecular hydrogen bonds along the polymer chain in chloroform and weak interactions in polar solvents, such as THF.

Influence of acid and base—Protonation and deprotonation of polymers: The precursor polymers **P1**–**P3** and the target polymers **P4**–**P6** were expected to react with protic acids and metal ions. The influence of acids and bases on the optical properties of the polymers is summarized in Table 4.

In the case of benzylated polymer **P1**, protonation in chloroform leads to a redshift of λ_{max} from 384 to 413 nm ($\Delta\lambda_{max}=29$ nm), and for the debenzylated polymer **P4**, $\Delta\lambda_{max}=10$ nm was observed on the addition of 20 mM CF_3COOH. This redshift may be attributable to planarization through hydrogen bonding (Figure 6) and charge transfer from the electron-rich phenyl ring to the electron-deficient pyridine moiety, which is enhanced by the protonation of nitrogen atoms of the pyridine ring.[29] Moreover, the formation of O···H–N^+ hydrogen bonds also enhances planarization, which is more evident in **P1** than in **P4** (Figure 6).

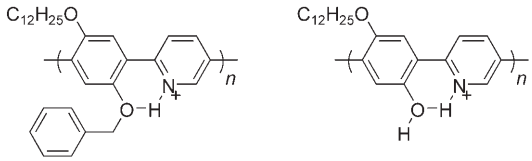

Figure 6. Possible structure of the protonated benzylated polymer (left) and the target polymer (right).

The difference in λ_{max} of the target polymers (debenzylated polymer) upon addition of acid is smaller compared with the precursor polymers (benzylated polymer). It indicates the presence of a strong interaction between the ether oxygen and the protonated pyridine nitrogen in the case of precursor polymers and large conformational changes and planarization caused by protonation. Such a significant redshift was also observed for other polymers (**P2**–**P6**). Figure 7 shows the influence of an acid on polymer **P1** and the influences of acid and base on polymer **P4**. Figure 8 depicts the changes in the emission spectra of polymer **P1** with increasing concentrations of CF_3COOH (0 to 400 mM). The emission intensities diminished rapidly with CF_3COOH concentration and all other polymers (**P1**–**P3**, **P5**–**P6**) showed similar changes in the absorption and emission properties.

In addition, the target polymers **P4**–**P6** are sensitive to sodium hydroxide on account of the presence of acidic hydroxyl groups on the polymer backbone. As seen in Figure 7, there is a significant blueshift ($\Delta\lambda_{max}$ of 45 nm) in the absorption maximum in the presence of base (20 mM NaOH) in a solution of **P4** in chloroform (Table 4). This was expected owing to the formation of electron-rich phenolate anions along the polymer backbone and the loss of planarization as a result of hydrogen bonding. Similar influences on the optical properties upon addition of acids were reported for pyridine-incorporated copolymers.[43] For the polymers **P4** to **P6**, the optical properties were different owing to hydrogen bonding between phenolic groups and the pyridine nitrogen atom as well as to the different substitution pattern of the pyridine ring. Moreover, all polymers are sensitive to the H^+ and OH^- ion concentrations. Thus the absorption and emission properties of the polymers can be fine-tuned over a wide range by varying the quantity of acid or base added.

Ionochromic effects of polymers: The metal-induced ionochromic effects of the bipyridine- or phenanthroline-incorporated conducting polymers have already been reported by a few research groups.[15,62–64] Owing to the good complexation ability of the pyridine nitrogen atom and adjacent phenolic OH groups, it was expected that polymers **P4**–**P6** would show significant responses to various metal ions. The iono-

Table 4. Influence of acid and base on the absorption/emission spectra of the polymers in chloroform.[a]

Polymer	Precursor polymers			Target polymers		
	P1	**P2**	**P3**	**P4**	**P5**	**P6**
$\lambda_{max}/\lambda_{emiss}$ [nm]	384/431	359/402	331/393	425/503	362/420	302/392
protonation, $\Delta\lambda$ [nm]	+29/+70 [b]	+8/+95 [b]	+12/+100 [b]	+10/+13	+5/+6	+6/+5
deprotonation, $\Delta\lambda$ [nm]				−45/−70	−10/−8	−6/−4

[a] + and − indicate red- and blueshifts, respectively. [b] No changes were expected owing to the absence of phenolic groups.

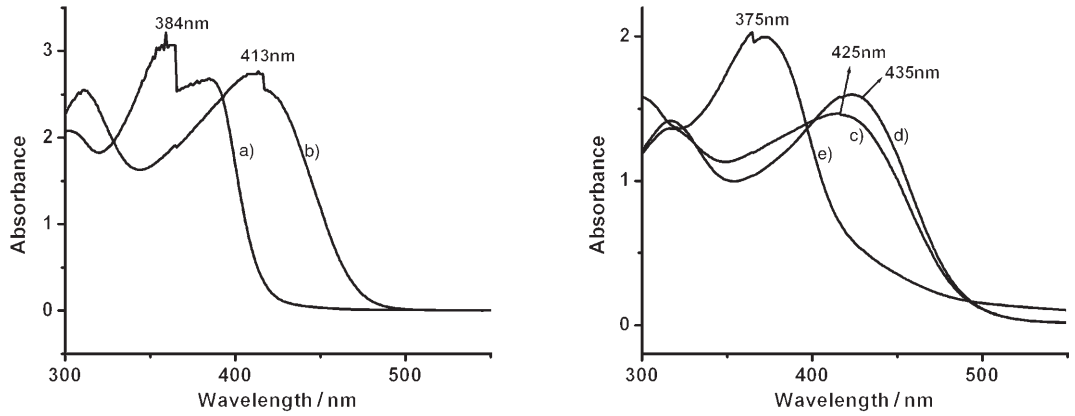

Figure 7. Absorption spectra in neutral pH for polymer **P1** (a) and **P4** (c), in the presence of H^+ for **P1** (b) and **P4** (d), in the presence of OH^- for polymer **P4** (e) in chloroform at room temperature. Concentrations of **P1** and **P4** were 3.06×10^{-5} M and 3.52×10^{-5} M, respectively. Note the redshift in λ_{max} caused by protonation and the blueshift caused by deprotonation. Absorbance has arbitrary units.

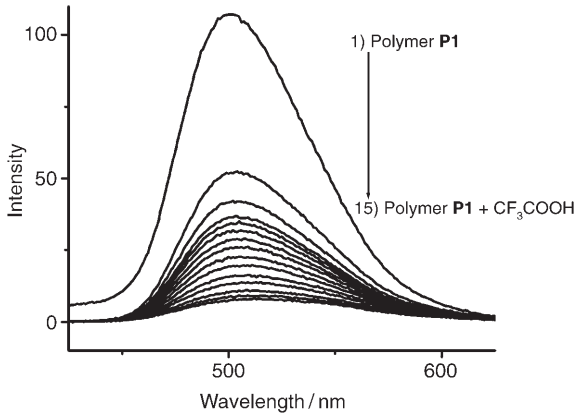

Figure 8. Changes in the emission spectra of **P1** in chloroform at different concentrations (in mM) of CF_3COOH: 1) 0, 2) 4, 3) 8, 4) 12, 5) 16, 6) 20, 7) 24, 8) 28, 9) 40, 10) 60, 11) 80, 12) 120, 13) 240, 14) 320, and 15) 400 mM in methanol. The concentration of **P1** was 3.06×10^{-5} M. Data of other polymers are given in the Supporting Information. Intensity has arbitrary units.

chromic effects of the polymers **P1**–**P6** were studied in THF with aliquots of solutions of the metal salts in methanol (Table 5). The colors vary from originally colorless/yellow to pink, green, purple, reddish brown, and so forth, depending on the metal ions and polymers used for analyses. The differences in the absorption ($\Delta\lambda_{max}$) of the polymers upon addition of metal ions are given in Table 5. The observed redshifts in the λ_{max} of the polymers were attributed to the conjugation enhancement along the polymer backbone induced by the coordination of metal ions with the pyridine nitrogen and the phenolic group.[15]

For different metal ions, the changes in λ_{max} may be attributed to the binding ability of the metal ions with the polymer backbone. Based on the spectral response, the precursor polymers (**P1**–**P3**) were only able to complex selected transition-metal ions, particularly Cu^{2+} and Fe^{3+} ions. In the case of polymer **P1**, the redshifts in the absorption were $\approx$35 nm and 146 nm upon the addition of Cu^{2+} and Fe^{3+} ion solutions, respectively. Similar influences of these metal ions were observed for the other two precursor polymers **P2** and **P3**. Thus, addition of metal salts completely quenched the fluorescence of polymers. This indicates strong coordination between the metal ions and the polymer.

The target polymers **P4**–**P6** showed significant changes in λ_{max} in the presence of Cu^{2+}, Fe^{3+}, Co^{2+}, and Ag^+ metal ions (see Table 5). Polymer **P4** showed more sensitivity towards metal ions, which may be caused by the adjacent position of the pyridine nitrogen atom and the phenolic group on the polymer backbone. Possible geometries of the metal complexes for **P1** and **P4** are given in Figure 9 (left). "Ln" represents other ligands or complexation sites from the adjacent polymer chains, as shown in Figure 9 (right).

Addition of a Cu^{2+} or Fe^{3+} salt solution to a solution of **P4** in THF resulted in a redshift ($\Delta\lambda_{max}$) of 44 and 144 nm, respectively. This is caused by the formation of metal complexes. In a few cases, the metal complexes showed a blueshift in their λ_{max} indicating that different metal ions demand different geometries in order to be able to form interchain complexes from adjacent polymer chains. This imposes considerable strain on the conformation of the polymer backbone (Figure 9). It is more pro-

Table 5. Absorption responses of **P1**–**P6** upon addition of metal ions in THF.

Polymer	λ_{max} [nm] of free ion	$\Delta\lambda_{max}$ [nm] in the presence of metal ions[a]									
		Cu^{2+}	Fe^{3+}	Co^{2+}	Ni^{2+}	Pd^{2+}	Mn^{2+}	Zn^{2+}	Ag^+	Mg^{2+}	Pr^{3+}
P1	384	+35	+146	[b]	[b]	[b]	[b]	[b]	−4	[b]	[b]
P2	362	+38	+72	[b]	[b]	[b]	[b]	[b]	[b]	[b]	[b]
P3	331	+64	+70	[b]	[b]	[b]	[b]	[b]	[b]	[b]	[b]
P4	383	+44	+144	+15	−6	−18	−5	−4	−13	−3	+8
P5	360	+49	+114	+4	[b]	[b]	[b]	[b]	−9	[b]	[b]
P6	302	+56	+20	+2	[b]	[b]	[b]	[b]	−3	[b]	[b]

[a] The + and − are red- and blueshifts, respectively. [b] No significant influence.

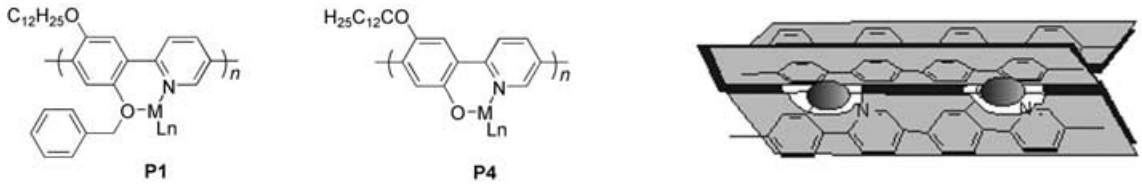

Figure 9. Representation of a possible structure of metal complexes of benzylated polymer **P1** and target polymer **P4** (left), and a sketch representing a possible structure of the polymer–metal complex inside the polymer lattice (right).

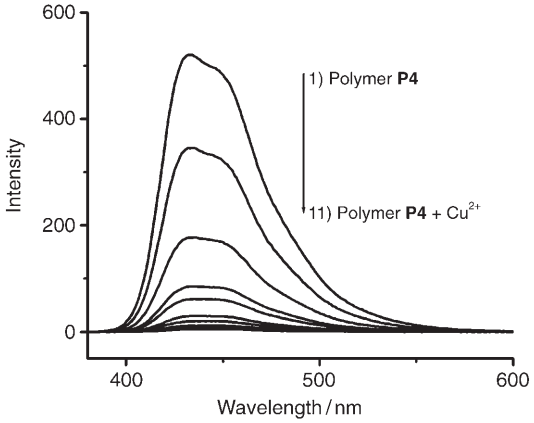

Figure 10. Changes in the emission spectra of **P4** in THF at different concentrations (in mM) of Cu^{2+} (methanolic solution): 1) 0, 2) 0.8, 3) 1.6, 4) 2.4, 5) 3.2, 6) 4.0, 7) 4.8, 8) 5.6, 9) 6.4, 10) 7.2, 11) 8.0 mM. The concentration of **P4** was 3.52×10^{-5} M. The spectral data of the other polymers are given in the Supporting Information. Intensity has arbitrary units.

nounced in the case of **P4**, in which two complexation sites from the adjacent rings participate in the complexation. Figure 10 depicts the emission spectra of polymer **P4** in THF in the presence of Cu^{2+} and the corresponding changes in fluorescence intensity with other transition-metal ions are shown in Figure 11.

A maximum quenching was observed in the presence of a solution of ~6 mM Cu^{2+} and ~1.6 mM Fe^{3+} ions. Polymer **P4** also showed significant changes in its optical properties

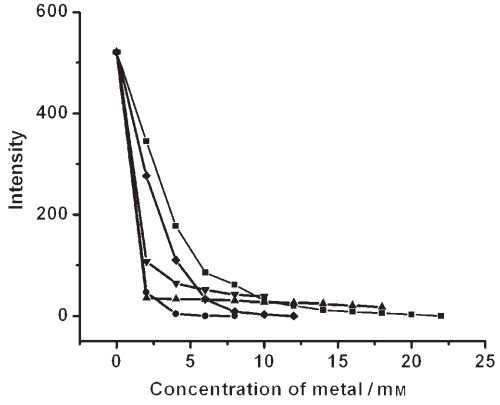

Figure 11. Titration traces of metal ions (Cu ■, Fe ●, Ag ▲, Ni ▼, Pd ◆) added to polymer **P4** in THF (concentration of **P4** is 3.52×10^{-5} M). Intensity has arbitrary units.

in the presence of other transition-metal ions, such as Co^{2+} ($\Delta\lambda_{max}=15$ nm), Ni^{2+} ($\Delta\lambda_{max}=6$ nm), Pd^{2+} ($\Delta\lambda_{max}=18$ nm), Ag^{+} ($\Delta\lambda_{max}=11$ nm), Mn^{2+} ($\Delta\lambda_{max}=5$ nm), and Zn^{2+} ($\Delta\lambda_{max}=4$ nm) (Table 4). There were no significant changes in λ_{max} in the presence of alkali, alkaline earth metals, or rare-earth metal ions. However, there was a slight change in the absorption maximum in the presence of Mg^{2+} ($\Delta\lambda_{max}=3$ nm) and Pr^{3+} ($\Delta\lambda_{max}=8$ nm) ions.

X-ray diffraction (XRD) studies: The XRD patterns of the powdered samples of polymers **P1**–**P6** were recorded to understand their self-assembly in the solid state. The typical X-ray patterns for polymers **P1** and **P4** are given in Figure 12. Precursor polymers **P1**–**P3** exhibited two peaks: a small peak in the low-angle region ($2\theta=5.50$–4.13 ($d=15.0$–21.0 Å)) which correspond to a distance between the polymer chains separated by the long alkoxy groups, and a broad peak in the wide-angle region of 2θ values at 21.02–21.80 ($d=4.0$–4.2 Å), which may be attributable to the side-to-side distance between loosely packed alkyl chains.[20,46] Thus, in the solid lattice, polymers are considered to be organized because the long alkoxy groups are able to crystallize. For the target polymers **P4**–**P6**, a broad peak at the wide-angle region of 2θ values at 20.80–23.12° was observed at $d=3.8$–4.2 Å.

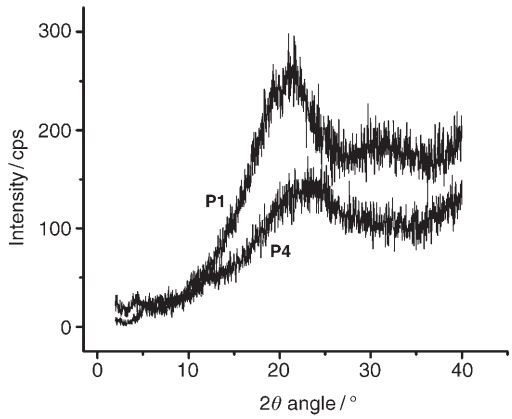

Figure 12. XRD patterns of polymers **P1** and **P4**. Data for the other polymers are given in the Supporting Information.

Conclusion

A series of luminescent conjugated polymers with alternating amphiphilic phenylene and pyridine units was synthesized by the Suzuki polycondensation method. All polymers exhibited good thermal properties, strong blue emissions in solution, and optimum solubility in common organic solvents, such as chloroform, THF, toluene, and trifluoroacetic acid. Significant changes in the optical properties were observed, depending upon the substitution of the pyridine ring (2,5-, 2,6-, or 3,5-) and the formation of intramolecular hydrogen bonds. The observed blueshift in the absorption and emission maxima observed for polymers **P4**–**P6** implies a reduction in planarization along the polymer backbone. The large Stokes shift in the values of λ_{max} and λ_{emiss} also confirmed the possibility of excited-state intramolecular proton transfer (ESIPT) for **P4** and **P5** that was facilitated by intramolecular hydrogen bonding. The optical properties of the polymers can be fine-tuned to a large extent by protonation, deprotonation, and the addition of metal ions. Addition of acid to the polymer solution gave a bathochromic shift and the presence of base showed a hypsochromic effect. In all the polymers, λ_{max} and λ_{emiss} exhibited metal-ion dependence. Therefore, the derived target polymers can be used for metal-ion sensors.

Experimental Section

Chemicals and instrumentation: All reactions were carried out under an inert atmosphere (N_2 or argon), unless specified otherwise. All reagents were purchased from Aldrich, Fluka, or Merck and were used without further purification, unless otherwise stated. All reactions were carried out with freshly distilled anhydrous solvents under an inert atmosphere. THF was purified by distillation over sodium under a nitrogen atmosphere. The ^{1}H and ^{13}C NMR spectra were collected on a Bruker ACF300 spectrometer operating at 300.135 and 75.469 MHz, respectively, in [D]chloroform or [D_4]methanol. Tetramethylsilane was used as an internal standard. FTIR spectra were recorded on a Bio-Rad FTS165 spectrophotometer in a KBr matrix. UV-visible spectra were recorded on a Shimadzu 3101 PC spectrophotometer and fluorescence measurements were carried out on a Shimadzu RF-5301 PC spectrofluorophotometer. Spectra were recorded in chloroform for polymers **P1**–**P5** and in methanol for **P6**. For metal complexation studies, the metal salt solution (in methanol or water) was mixed with polymer solution in THF. Thermogravimetric analyses were performed on TA Instruments SDT2960 with a heating rate of 10 °C min^{-1} under a nitrogen atmosphere. Gel permeation chromatography (GPC) was used to obtain the molecular weight of the polymers with reference to polystyrene standards with THF as the eluant. X-ray powder diffraction patterns were obtained on a Siemens D5005 X-ray diffractometer with $Cu_{K\alpha}$ (1.54 Å) radiation (40 kV, 40 mA). Samples were mounted on a sample holder and scanned between $2\theta = 2$–40° with a step size of $2\theta = 0.01$°. Cyclic voltammetry (CV) was performed on an EG&G Princeton model 273 A potentiostat/galvanostat system with a three-electrode cell in a solution of Bu_4NClO_4 (0.10 M) in acetonitrile as the electrolyte, with an Ag/AgCl reference electrode, a platinum wire as the counterelectrode, and a glassy carbon electrode as the working electrode at a scan rate of 50 mV s^{-1}.

Synthesis: The synthetic strategy for polymers **P1**–**P6** is shown in Scheme 1. 2,5-Dibromo hydroquinone (**2**), 2,5-dibromo-4-dodecyloxyphenol (**3**), 2,5-dibromo-1-benzyloxy-4-dodecyloxybenzene (**4**), and 1-benzyloxy-4-dodecyloxyphenyl-2,5-bis(boronic acid) (**5**) were synthesized by means of the standard procedure reported in the literature.[47,51]

General procedure for the polymerization of precursor polymers P1–P3: Compound **5** (4.11 g, 9 mmol) and dibromopyridine (2.14 g, 9 mmol) were dissolved in degassed toluene (90 mL) under a nitrogen atmosphere. After the addition of an aqueous solution of K_2CO_3 (2 M, 60 mL), the catalyst tetrakis(triphenylphosphino)palladium(**0**) (3 mol %, 0.52 g) was added, and the mixture was stirred vigorously for 72 h at 85–90 °C, cooled to room temperature, and poured into methanol (1 L). The yellow solid was filtered, washed with 1) water, 2) methanol (2×25 mL), and 3) acetone (3×25 mL). The crude product was purified by repeated precipitation from methanol. The observed low molecular weight may have been caused by fractionation of soluble components during GPC.

Polymer P1: Bright yellow powder; yield 83 %; ^{1}H NMR ($CDCl_3$): $\delta =$ 8.99 (d, 1H; py-H), 8.18 (m, 1H; py-H), 8.03 (m, 1H; py-H), 7.90 (b, 2H; Ar-H), 7.48 (b, 5H; Ar-H), 5.24 (b, 2H; PhOCH_2Ph), 4.10 (b, 2H; PhOCH_2CH$_2$-), 1.80 (b, 2H; -OCH$_2$CH_2-), 1.30 (b, 18H; -CH$_2$-(CH_2)$_9$CH$_3$), 0.90 ppm (b, 3H; -CH$_3$); ^{13}C NMR ($CDCl_3$): $\delta =$ 149.5, 138.1, 136.4, 128.4, 127.8, 127.4, 127.2, 71.8, 69.4, 31.8, 29.6, 26.0, 22.6, 14.0 ppm; FTIR (KBr): $\tilde{\nu} =$ 3062, 2922, 2852, 1590, 1504, 1459, 1420, 1359, 1230, 1197, 1024, 843, 732, 694 cm^{-1}.

Polymer P2: Yellow solid; yield 86 %; ^{1}H NMR ($CDCl_3$): $\delta =$ 8.04 (b, 1H; py-H), 7.90 (m, 2H; py-H), 7.71–7.30 (b, 7H; Ar-H), 5.21 (b, 2H; PhOCH_2Ph), 4.14 (b, 2H; PhOCH_2CH$_2$-), 1.81 (b, 2H; -OCH$_2$CH_2-), 1.30 (b, 18H; -CH$_2$(CH_2)$_9$CH$_3$), 0.86 ppm (b, 3H; -CH$_3$); ^{13}C NMR ($CDCl_3$): $\delta =$ 159.7, 154.4, 151.5, 128.3, 127.5, 123.6, 71.6, 31.8, 29.5, 26.3, 22.6, 14.0 ppm; FTIR (KBr): $\tilde{\nu} =$ 3061, 2923, 2852, 1567, 1503, 1451, 1379, 1196, 1022, 814, 734, 694 cm^{-1}.

Polymer P3: Light brown solid; yield 73 %; ^{1}H NMR ($CDCl_3$): $\delta =$ 8.85 (b, 2H; py-H), 8.17 (b, 1H; py-H), 7.70–7.10 (m, 6H; Ar-H), 5.10 (b, 2H; PhOCH_2Ph), 3.94 (b, 2H; PhOCH_2CH$_2$-), 1.77 (b, 2H; -OCH$_2$CH_2-), 1.22 (b, 18H; -CH$_2$(CH_2)$_9$CH$_3$), 0.87 ppm (b, 3H; -CH$_3$); ^{13}C NMR ($CDCl_3$): $\delta =$ 150.9, 149.9, 148.7, 137.5, 136.7, 133.1, 128.5, 127.8, 127.1, 116.8, 115.5, 71.8, 69.5, 31.8, 29.6, 26.0, 22.6, 14.0 ppm; FTIR (KBr): $\tilde{\nu} =$ 3032, 2923, 2852, 1946, 1744, 1589, 1507, 1436, 1378, 1267, 1201, 1022, 863, 729 cm^{-1}.

General syntheses of polymers P4–P6: Precursor polymer **P1** (2.80 g) was dissolved in a mixture of $CHCl_3$/THF/EtOH (100:50:30 mL) at room temperature. 10 % Pd/C (5.0 g) and three drops of concentrated HCl were added, and the mixture was flushed with nitrogen gas. The flask was fitted with a hydrogen gas balloon and the mixture was stirred at room temperature for about 2–3 days and then filtered through silica gel/celite. The filtrate was concentrated under reduced pressure. The concentrated solute was precipitated from methanol, filtered, and washed with 1) methanol, 2) acetone.

Polymer P4: Dark brown solid; yield 82 %; ^{1}H NMR ($CDCl_3$/CF_3COOD): $\delta =$ 9.02 (b, 1H; py-H), 8.82 (b, 1H; py-H), 8.35 (b, 1H; py-H), 7.66 (b, 1H; Ar-H), 7.30 (b, 1H; Ar-H), 4.17 (b, 2H; PhOCH_2CH$_2$-), 1.91 (b, 2H; -OCH$_2$CH_2-), 1.31 (b, 18H; -CH$_2$(CH_2)$_9$CH$_3$), 0.92 ppm (b, 3H; -CH$_3$); ^{13}C NMR ($CDCl_3$): $\delta =$ 190.7, 149.8, 136.8, 131.8, 128.5, 128.4, 127.8, 127.2, 71.8, 31.8, 29.6, 26.0, 22.6, 14.0, 6.6 ppm; FTIR (KBr): $\tilde{\nu} =$ 3408, 3061, 2923, 2852, 2037, 1945, 1591, 1545, 1505, 1462, 1417, 1219, 1017, 844, 734, 696 cm^{-1}.

Polymer P5: Dark brown solid; yield 85 %; ^{1}H NMR ($CDCl_3$): $\delta =$ 9.80 (s, 1H; py-H), 8.00 (b, 1H; py-H), 7.87 (b, 1H; py-H), 7.71 (b, 1H; Ar-H), 7.46 (s, 1H; Ar-H), 4.14 (b, 2H; PhOCH_2CH$_2$-), 1.78 (b, 2H; -OCH$_2$CH_2-), 1.26 (b, 18H; -CH$_2$(CH_2)$_9$CH$_3$), 0.86 ppm (b, 1H; -CH$_3$); ^{13}C NMR ($CDCl_3$): $\delta =$ 191.0, 190.0, 159.5, 134.5, 128.4, 128.3, 127.4, 125.4, 63.2, 31.7, 29.5, 26.1, 22.5, 13.9, 6.9 ppm; FTIR (KBr): $\tilde{\nu} =$ 3437, 3059, 2923, 2852, 1567, 1505, 1451, 1375, 1198, 1020, 812, 733, 695 cm^{-1}.

Polymer P6: Dark brown solid; yield 76 %; ^{1}H NMR ([D_7]DMF/CF_3COOD): $\delta =$ 10.35 (b, 1H; py-H), 10.24 (b, 1H; py-H), 9.10 (b, 1H; py-H), 7.36 (b, 1H; Ar-H), 6.95 (b, 1H; Ar-H), 4.31 (s, 2H; PhOCH_2CH$_2$-), 1.82 (b, 2H; -OCH$_2$CH_2-), 1.25 (b, 18H; -CH$_2$-(CH_2)$_9$CH$_3$), 0.86 ppm (b, 1H; -CH$_3$); ^{13}C NMR (CD_3OD): $\delta =$ 163.8, 151.4, 151.1, 147.9, 130.4, 129.3, 128.2, 128.0, 126.1, 117.3, 70.3, 62.0, 35.4, 31.3, 23.7, 14.5 ppm; FTIR (KBr): $\tilde{\nu} =$ 3406, 2925, 2854, 1638, 1507, 1455, 1383, 1204, 1057, 1022, 868, 737, 698 cm^{-1}.

Acknowledgements

We thank the Singapore-MIT Alliance for a research fellowship and financial assistance. The technical support from the Department of Chemistry, National University of Singapore, is also acknowledged.

[1] K. Müllen, G. Wegner, *Electronic Materials: The Oligomer Approach*, Wiley-VCH, Weinheim, Germany, **1998**.
[2] *Handbook of Conducting Polymers* (Eds.: A. Skotheim, R. L. Elsenbaumer, J. R. Reynolds), Marcel Dekker, New York, **1997**.
[3] Z. L. Li, S. C. Yang, H. F. Meng, Y. S. Chen, Y. Z. Yang, C. H. Liu, S. F. Horng, S. Hsu, L. C. Chen, J. P. Hu, R. H. Lee, *Appl. Phys. Lett.* **2004**, *84*, 3558–3560.
[4] A. Kraft, A. C. Grimsdale, A. B. Holmes, *Angew. Chem.* **1998**, *110*, 416–443; *Angew. Chem. Int. Ed.* **1998**, *37*, 402–428.
[5] R. H. Friend, R. W. Gymer, A. B. Holmes, J. H. Burroughes, R. N. Marks, C. Taliani, D. D. C. Bradley, D. A. Dos Sontos, J. L. Brédas, M. Lögdlund, W. R. Salaneck, *Nature* **1999**, *397*, 121–128.
[6] U. H. F. Bunz, *Chem. Rev.* **2000**, *100*, 1605–1644, and references therein.
[7] Q. Peng, Z. Y. Lu, Y. Huang, M. G. Xie, D. Xiao, S. H. Han, J. B. Peng, Y. Cao, *J. Mater. Chem.* **2004**, *14*, 396–401.
[8] D. T. McQuade, A. E. Pullen, T. M. Swager, *Chem. Rev.* **2000**, *100*, 2537–2574.
[9] X. Gong, R. R. Matthew, J. C. Ostrowski, D. Moses, G. C. Bazan, A. J. Heeger, *Adv. Mater.* **2002**, *14*, 581–585.
[10] J. M. Tour, *Acc. Chem. Res.* **2000**, *33*, 791–804.
[11] G. Yu, J. Gao, J. C. Hummelen, F. Wudl, A. J. Heeger, *Science* **1995**, *270*, 1789–1791.
[12] Y. Yao, J. J. S. Lamba, J. M. Tour, *J. Am. Chem. Soc.* **1998**, *120*, 2805–2810.
[13] A. Godt, A. D. Schluter, *Adv. Mater.* **1991**, *3*, 497–499.
[14] J. Roncali, *Chem. Rev.* **1997**, *97*, 173–206.
[15] B. Liu, W. L. Yu, J. Pei, S. Y. Liu, Y. H. Lai, W. Huang, *Macromolecules* **2001**, *34*, 7932–7940.
[16] B. L. Lee, T. Yamamoto, *Macromolecules* **1999**, *32*, 1375–1382, and references therein.
[17] H. Wang, R. Helgeson, B. Ma, F. Wudl, *J. Org. Chem.* **2000**, *65*, 5862–5867.
[18] J. Pei, X. L. Liu, W. L. Yu, Y. H. Lai, Y. H. Niu, Y. Cao, *Macromolecules* **2002**, *35*, 7274–7280.
[19] C. G. Bangcuyo, M. E. Rampey-Vaughn, L. T. Quan, S. M. Angel, M. D. Smith, U. H. F. Bunz, *Macromolecules* **2002**, *35*, 1563–1568.
[20] T. Yamamoto, Q. Fang, T. Morikita, *Macromolecules* **2003**, *36*, 4262–4267.
[21] K. Pieterse, J. A. J. M. Vekemans, H. Kooijiman, A. L. Spek, E. W. Meijer, *Chem. Eur. J.* **2000**, *6*, 4597–4603.
[22] Q. T. Zhang, J. M. Tour, *J. Am. Chem. Soc.* **1997**, *119*, 9624–9631.
[23] Z. H. Zhou, T. Maruyama, T. Kanbara, T. Ikeda, K. Ichimura, T. Yamamoto, K. Tokuda, *J. Chem. Soc. Chem. Commun.* **1991**, 1210–1211.
[24] T. Morikita, I. Yamguchi, T. Yamamoto, *Adv. Mater.* **2001**, *13*, 1862–1864.
[25] C. J. Tonzola, M. M. Alam, S. A. Jenekhe, *Adv. Mater.* **2002**, *14*, 1086–1092.
[26] S. C. Yu, S. Hou, W. K. Chan, *Macromolecules* **1999**, *32*, 5251–5256.
[27] B. L. Lee, T. Yamamoto, *Macromolecules* **2002**, *35*, 2993–2999.
[28] E. J. Samuelsen, A. P. Monkman, L. A. A. Pattersson, L. E. Horsburgh, K. E. Aasmundtveit, S. Ferrer, *Synth. Met.* **2001**, *124*, 393–398.
[29] D. K. Fu, B. Xu, T. M. Swager, *Tetrahedron* **1997**, *53*, 15487–15494.
[30] M. Bacquet, B. Martel, M. Morcellet, K. I. Benabadji, K. Medjahed, A. Mansri, A.-H. Meniai, M. B. Lehocine, *Mater. Lett.* **2003**, *58*, 455–459.
[31] Y. Z. Wang, A. J. Epstein, *Acc. Chem. Res.* **1999**, *32*, 217–224.
[32] A. J. Epstein, J. W. Blatchford, Y. Z. Wang, S. W. Jessen, D. D. Gebler, L. B. Lin, T. L. Gustafson, H. L. Wang, Y. W. Park, T. M. Swager, *Synth. Met.* **1996**, *78*, 253–261.
[33] C. Wang, M. Kilitziraki, J. A. McBride, M. R. Bryce, L. E. Horsburgh, A. K. Sheridan, A. P. Monkman, I. D. W. Samuel, *Adv. Mater.* **2000**, *12*, 217–222.
[34] F. Babudri, G. M. Farinola, F. Naso, *J. Mater. Chem.* **2004**, *14*, 11–34.
[35] D. A. P. Delnoye, R. P. Sijbesma, J. A. J. M. Vekemans, E. W. Meijer, *J. Am. Chem. Soc.* **1996**, *118*, 8717–8718.
[36] H. A. M. Van Mullekom, J. A. J. M. Vekemans, E. W. Meijer, *Chem. Commun.* **1996**, 2163–2164.
[37] S. K. Pollack, Y. M. Hijji, B. Kgobane, *Macromolecules* **1997**, *30*, 6709–6711.
[38] D. J. Sikkema, *Polymer* **1998**, 5981–5986.
[39] J. L. Burkett, T. D. Dang, F. E. Arnold, L. S. Tan, *Polymer* **1997**, *38*, 131–132.
[40] T. Kanbara, N. Saito, T. Yamamoto, K. Kubato, *Macromolecules* **1991**, *24*, 5883–5885.
[41] C. J. DuBois, J. R. Reynolds, *Adv. Mater.* **2002**, *14*, 1844–1846.
[42] P. H. Aubert, M. Knipper, L. Groenendaal, L. Lutsen, J. Manca, D. Vanderzande, *Macromolecules* **2004**, *37*, 4087–4098.
[43] S. C. Ng, H. F. Lu, H. S. O. Chan, A. Fujii, T. Laga, K. Yoshino, *Adv. Mater.* **2000**, *12*, 1122–1125, and references therein.
[44] Y. Z. Wang, D. D. Gebler, D. K. Fu, T. M. Swager, A. G. MacDiarmid, A. J. Epstein, *Synth. Met.* **1997**, *85*, 1179–1182.
[45] A. P. Monkman, L. O. Pålsson, R. W. T. Higgins, C. Wang, M. R. Bryce, A. S. Batsanov, J. A. K. Howard, *J. Am. Chem. Soc.* **2002**, *124*, 6049–6055.
[46] T. Yasuda, T. Yamamoto, *Macromolecules* **2003**, *36*, 7513–7519.
[47] C. Baskar, Y. H. Lai, S. Valiyaveettil, *Macromolecules* **2001**, *34*, 6255–6260, and references therein.
[48] W. Ji, H. I. Elim, J. He, F. Fitrilawati, C. Baskar, S. Valiyaveettil, W. Knoll, *J. Phys. Chem. B* **2003**, *107*, 11043–11047.
[49] R. Renu, S. Valiyaveettil, C. Baskar, A. Putra, F. Fitrilawati, W. Knoll, *MRS Proc.* **2003**, *776*, 201–202.
[50] W. Shu, S. Valiyaveettil, *Chem. Commun.* **2002**, 1350–1351.
[51] L. F. Tietze, Th. Eicher, *Reactions and Syntheses in the Organic Chemistry Laboratory*, University Science, Mill Valley, CA, **1989**, p. 253.
[52] M. Kreyenschmidt, F. Uckert, K. Müllen, *Macromolecules* **1995**, *28*, 4577–4582.
[53] R. Cervini, X.-C. Li, G. W. C. Spencer, A. B. Holmes, S. C. Moratti, R. H. Friend, *Synth. Met.* **1997**, *84*, 359–360.
[54] S. C. Ng, H. F. Lu, H. S. O. Chan, A. Fujji, T. Laga, K. Yoshino, *Macromolecules* **2001**, *34*, 6895–6903.
[55] D. M. De Leeuw, M. M. J. Simenon, A. R. Brown, R. E. F. Einerhand, *Synth. Met.* **1997**, *87*, 53–59.
[56] T. Yamamoto, Z. H. Zhou, T. Kanbara, M. Shimura, K. Kizu, T. Maruyama, Y. Nakamura, T. Fukuda, B. L. Lee, N. Ooba, S. Tomaru, T. Kurihara, T. Kaino, K. Kubota, S. Sasaki, *J. Am. Chem. Soc.* **1996**, *118*, 10389–10399.
[57] A. Douhal, F. A. Guerri, U. A. Acuña, *J. Phys. Chem.* **1995**, *99*, 76–80.
[58] R. M. Tarakka, X. Zhang, S. A. Jenekhe, *J. Am. Chem. Soc.* **1996**, *118*, 9438–9439.
[59] M. A. Ríos, M. C. Ríos, *J. Phys. Chem. A* **1998**, *102*, 1560–1567.
[60] J. C. Penedo, M. Mosquera, F. R. Prieto, *J. Phys. Chem. A* **2000**, *104*, 7429–7441.
[61] L. M. Tolbert, K. M. Solntsev, *Acc. Chem. Res.* **2002**, *35*, 19–27.
[62] B. Wang, M. R. Wasielewski, *J. Am. Chem. Soc.* **1997**, *119*, 12–21.
[63] T. Yasuda, I. Yamaguchi, T. Yamamoto, *Adv. Mater.* **2003**, *15*, 293–296.
[64] M. Zhang, P. Lu, Y. Ma, J. Shen, *J. Phys. Chem. B* **2003**, *107*, 6535–6538.

Received: January 24, 2005
Published online: June 23, 2005

